Mechanical Modeling of Indigo's Printing Machine Parts

Nurith Schupper, Peter Forgacs and Wael Salalha; Materials R&D, Hewlett-Packard Indigo, Rehovot, Israel

Abstract

We develop methods to predict printing machines components behavior in order to reduce cost, shorten production time, and to improve lifespan and print quality. These methods of optimization are based on finite element calculations using Abaqus program. Specifically, we model HP-Indigo's machine units, such as the printing blanket, an ink dispersion unit seal and a substrate coating unit. For each component we first characterize the materials by off-line measurements and propose appropriate material descriptions. Then the system is analyzed and dependence of its behavior on relevant parameters is found. This allows for optimization and proposing future configurations, where expensive and time consuming prototypes can be built and tested only for most preferable candidates. These methods are very interesting for a wide range of applications.

Introduction

Developing a new printing machine is a very challenging task. The performance of the machine must be higher compared to the old one and therefore designers must take into account all relevant consumers expectations. Using only empirical methods can be quite expensive and time consuming. In contrast, modern simulation tools allow solutions which enable reaching both costs and development time. Another advantage of using simulations is that one can easily increase the amount of test data. During the last years the performance of computers has increased rapidly and also commercial finite element analysis (FEA) programs have increased capabilities and robustness so that it is possible to analyze big and nonlinear models [1]. One important example is the tire industry where such modeling is most widely used [2]. FEA of vehicles and tires has become a very important aspect of tire design and failure analysis to most companies. The method offers a predictive capability for design where more and more realistic models are developed for various rolling conditions. Such simulations have much helped in improving tires durability and reliability. For rubbery printing blankets, however, although some theoretical studies were done [3], there are almost no FEA simulation treatments up to date. This is mainly a result of the complexity of these systems due to contact complications and due to nonlinearity and time dependence of thin rubbery layers forming the blankets. In addition, as mentioned, FEA programs were not as sophisticated in the past leading to much more effort in element programming and much less capability of providing complicated systems results. Here we describe several models of machine parts which are analyzed with Abaqus program. We show that by using Abaqus FEA we can overcome these solution barriers, obtain physical insight and propose optimal design configurations for printing machines parts.

The paper is organized as follows: First we describe Indigo's printing process and the use of the printing blanket. The printing blanket will be the main modeling part described here to which we will focus most of our attention. We discuss the blanket structure and offline characterization methods to obtain models for the materials comprising the blanket. Next we describe modeling in various techniques: a static symmetric model, a static a-symmetric model and a steady-state rolling model. These will be employed to model three different blanket failures which will be described. We show how with the simulation aid we can predict which configurations are preferable for failure elimination. In the following sections we describe two other systems simulated: a seal for ink grinding unit optimized by employing Abaqus modeling and a substrate coating unit composed of two rubbery cylinders. Finally some general conclusions and remarks are presented.

Parts Modeling

HP-Indigo's Printing Blanket

HP-Indigo's Process and Blankets Used

Indigo's unique digital offset printing combines between digital electrophotographic imaging and offset lithography printing based on liquid ink. This allows for both electronic printing on demand and obtaining the best quality offset printing on a wide variety of substrates. The electrophotographic process (which is also used in almost all laser printers and copying machines) is based on selectively charging regions of an organic photoconductor drum (OPC) as depicted in figure 1. The OPC (insulating in dark and conducting in light) is homogeneously negatively charged on its surface by contact with a charge roller. Then illuminating it creates electron-hole pairs. Holes transverse film and eliminate surface charge, to create a latent image. In regular electrophotography the next step consists of creating a visible image by exposing triboelectrically charged toner particles to the OPC. These particles are attracted to the charged regions and the formed image is then transferred from the OPC drum to an oppositely charged paper. Different from this, in the Indigo process, the liquid electroink which adheres to the discharged OPC regions is first transferred (1st Transfer, T1) to an intermediate flexible carrier, a rubber blanket and only after that it is transferred to the paper (2nd Transfer, T2). The blanket conforms to the local topography of the substrate thus ensuring good transfer. It compensates for any unevenness of the substrate surface by enabling ink to reach the bottom of any depressions or grain. In other words it acts as a shock absorber and pressure pad ensuring ink transfer from blanket to substrate. In addition, the blanket protects the surface of the OPC from wear due to friction. Upon transfer from the OPC the image is $5\mu m$ thick and mostly liquid and after being heated on the blanket (~100^0C) the ink is $1\mu m$ thick and mostly solid (on being transferred to substrate). The 2nd Transfer, T2, from blanket to paper is mainly due to mechanical (pressure) forces.

 ©2014 Society for Imaging Science and Technology

The blanket consists of multiple thin connected viscoelastic layers positioned on a rigid cylindrical drum. The simulations shown here aim at predicting blanket behavior at the nip contacts, T1 contact with the OPC and T2 contact with the impression drum under various conditions. These conditions may be either dry or wet contact, either with or without paper (for T2 contact), or contact with paper edge or punch due to jams etc. The goal is to understand mechanical failures occuring in these nips and to optimize blanket layers and process parameters in order to increase its lifespan and print quality.

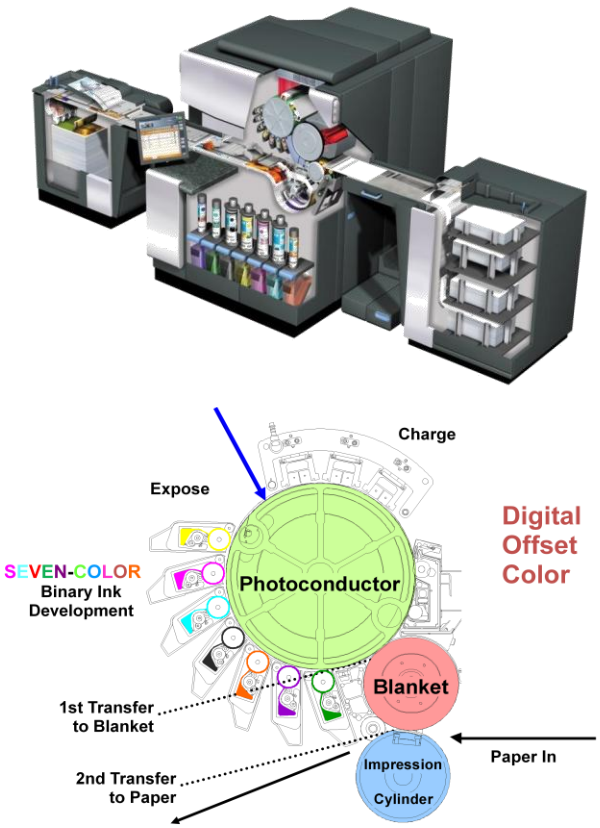

***Figure 1**. (a) A picture of an HP-Indigo machine (b) The Indigo process where an intermediate transfer medium, the blanket, is used between the OPC and the paper impression cylinder.*

The blanket consists of several layers (see Figure 2) of which we are interested in three: the Compressible Layer (CL), which is composed out of foam rubber, and the Top Conductive Layer (TCL) and the Compressible Soft Layer (CSL) which are rubbery layers.

There are two main groups of Indigo machines which differ by the type of paper-handling mechanism they work with: Sheetfed (or cut-sheet) or Webfed (or roll-fed e.g. for labels and flexible packaging). For these different machines and processes there are two different blankets made out of different materials and at different technologies (though their general structure is the same as described above). These two blankets are named here according to the corresponding machine type.

Blanket Materials Descriptions

The mechanical properties of the three modeled layers are measured and will be described in what follows.

(a)

(b)

***Figure 2**. (a) A picture of HP-Indigo's blanket (b) Schematic cross-section illustration of blankets layers.*

Samples of CSL and TCL (rubbers) were measured by static DMA indentation. The force vs. deflection curves were fitted to a Mooney-Rivlin (MR) model by adjusting the material parameters. The MR model is chosen since it captures high strains better than the Neo-Hookean model and because it is the simplest model with a minimum number of parameters which describes well many types of rubber. The strain energy function is given by

$$W = \underbrace{C_{10}\left[\left(\lambda_1\lambda_2\lambda_3\right)^{-\frac{2}{3}}\left(\lambda_1^2+\lambda_2^2+\lambda_3^2-3\right)\right]}_{Deviatoric} \quad (1)$$

$$+\underbrace{C_{01}\left[\left(\lambda_1\lambda_2\lambda_3\right)^{-\frac{4}{3}}\left(\lambda_1^2\lambda_2^2+\lambda_2^2\lambda_3^2+\lambda_3^2\lambda_1^2-3\right)\right]}_{Deviatoric}+\underbrace{D_1^{-1}(\lambda_1\lambda_2\lambda_3-1)^2}_{Volumetric}$$

where C_{01}, C_{10}, D_1 are material constants and

λ_i – i=1,2,3 are principle stretches in the different directions.

For consistency with linear elasticity the fitted parameters have to obey the following relations with the low strain values

$$C_{01}+C_{10}=\frac{\mu}{2}=\frac{1}{2}\cdot\frac{E}{2(1+\nu)} \quad (2)$$

$$D_1=\frac{2}{\kappa}=2\cdot\frac{3(1-2\nu)}{E} \quad (3)$$

where μ – is the shear modulus and

κ – is the bulk modulus and

E and ν are the Young's modulus and the Poisson's ratio respectively.

Most rubbers are almost incompressible and therefore the Poisson ratio is assumed as ~0.49. Inserting this we find that the parameters fitted both for the CSL and for the TCL are compatible with the elastic linear values known from the manufacturer and also measured by nanoindentation.

Compressibility of the CL layer (foam rubber) was measured by Instron (Figure 3) and Abaqus hyperfoam [1] model (N=2) was fitted. Both sheet-fed and web blankets were measured and fitted with the same functional form though different parameters were used.

Different from hyperelastic materials where several built-in functional forms are proposed, for foam materials there is only one model available:

$$W=\sum_{i=1}^{N}\frac{2\mu_i}{\alpha_i^2}\left\{\underbrace{\left(\lambda_1^{\alpha_i}+\lambda_2^{\alpha_i}+\lambda_3^{\alpha_i}-3\right)}_{\text{deviatoric = shear}}+\underbrace{\beta_i^{-1}\left[\left(\lambda_1\lambda_2\lambda_3\right)^{-\alpha_i\beta_i}-1\right]}_{\text{dilitation = volumetric}}\right\} \qquad (4)$$

where α_i, μ_i, β_i – are material constants.
The degree of compressibility is related to the Poisson ratio by

$$\beta_i=\nu_i/(1-2\nu_i) \qquad (5)$$

Similar to the previous procedure, for consistency with linear elsticity the coefficients have to relate to the low strain measured values:

Initial shear modulus $\quad \mu_0=\sum_{i=1}^{N}\mu_i \qquad (6)$

Initial bulk modulus $\quad \kappa_0=\sum_{i=1}^{N}2\mu_i(1/3+\beta_i) \qquad (7)$

and found to fit them.

Changing the coefficient of friction does not vary much the results since the Poisson's ratio of the foam is close to 0. Therefore, compression in the *z* axis does not yield strains in the *x,y* axis and the Instron data gives uniaxial strain mode with no further corrections required.

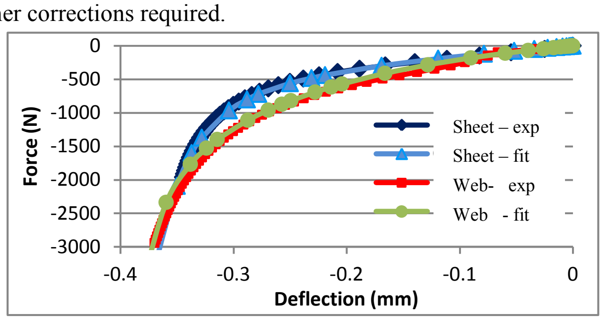

***Figure 3**. Force vs. deflection curve of sheet and web CL layer and fitting experimental results with curve (3)*

Rubber exhibits further special mechanical behavior such as viscoelasticity, (time dependent elasticity) and hysteresis (different stress-strain relationships during unloading). In addition, in rubbery materials damage or Mullin's effect may occur, i.e. the stiffness decreases after multiple loading and unloading cycles. Further dynamical compression experiments were conducted with many cycling repetitions and at a greater rate. From these experiments it was obtained that the material reaches a constant hysteresis loop after preconditioning. A new constitutive model equation was developed and fitted for this preconditioned hysteresis loop and its implementation as a new material model in Abaqus is underway [4].

Static Model for T1 – Solid Printing Differences

T1 contact consists of two cylinders compression. The OPC is modeled as a thin elastic layer made of Aluminum and PET and placed on a rigid drum. The blanket is modeled as a thin multiple layer composed of the materials above and also positioned on a rigid drum. 2D plane strain assumption (valid for long cylinders) (Figure 4a) is employed with additional *x* axis symmetry for a static model. Blanket and OPC initially touch at a point and then a constant deflection is forced ranging between 20µm and 380µm (Figure 4b).

We obtain pressure profiles for each blanket type at every deflection value (Figure 5). In order to validate the results we measure the pressure profiles by an I-scan detector on the press machine. For small deflections we find that the pressure profiles follow Hertz model [5] behavior $P(x)=P_0\sqrt{1-(x/x_0)^2}$, as expected for two cylinders exhibiting linear elastic behaviour. For higher compression values the profile center greatly increases and this occurs due to the strong nonlinearity of the hyperfoam as seen from the sress-strain curves of Figure 3.

(a)

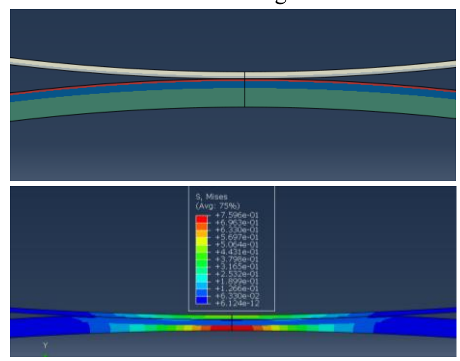

(b)

***Figure 4**. (a) Blanket and OPC initial contact (b) Von-Mises stresses picture after 380µm compression*

Although the qualitative behavior of both blanket types is similar, Web presses blanket pressure profiles have much larger values for the same deflections (peak about 2.3 times greater). This explains differences upon solid printing where sheet fed blankets show a failure of white regions due to lack of ink transfer while web blankets transfer well. The much lower pressure profile of sheet-fed presses ends in a decrease of transfer at T1. This failure is directly connected to ink consumption and by optimization we can reach significant improvement.

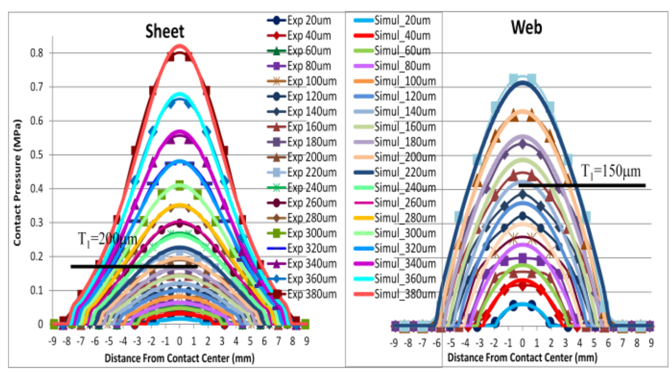

***Figure 5**. T1 contact pressure profiles between OPC and blanket for 20µm-380µm deflections (a) for sheet-fed presses (b) for web presses. Horizontal lines show T1 contact values for both types of blankets showing much greater T1 pressures for sheet-fed blankets.*

Static Model for T2 – Paper Size Marks

Another blanket failure is Paper Size Marks (PSM) which occurs after printing on many small papers and then on larger ones. At the position of the small paper edge, ink does not transfer well to the blanket. This was studied and found to be a result of blanket top layer wear. We would like to understand the effect of layers structure on the top layer abrasion. We simulate T2 contact with

©2014 Society for Imaging Science and Technology

paper edge and probe blanket deformation after the edge punch (Figure 6c). The paper is placed on a carton and its edge is rounded to avoid singularities. This is validated by microscopic studies where the edge radius of 10-20μm was measured. Both paper and carton are considered elastic with a high modulus. In this case plane strain assumption is used though symmetry around the *x* axis is no longer valid.

(a)

(b)

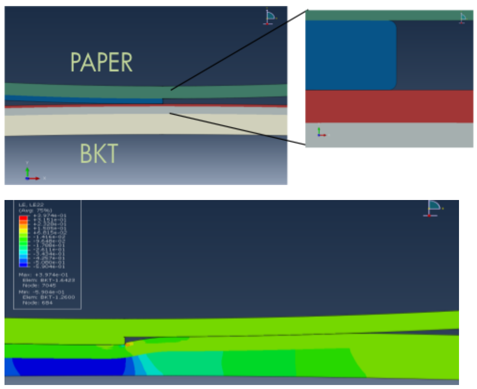

***Figure 6**. Von-Mises stresses (a) before and (b) after 200μm compression with paper edge.*

After edge punch the top CSL layer is greatly deformed exhibiting very large strains. We assume that the extent of damage is proportional to the maximum contact pressure on the blanket. This assumption follows Archard's theory and related wear models [6] and is based on the theory of asperity contact that the volume of the removed debris due to wear is proportional to the work done by friction forces. Going along the contact line, the pressure acquires a maximum and for an optimal configuration we wish that this value be smallest possible.

The following parameters were tested as contributing to PSM formation: T2 pressure, all layers thicknesses and all layers hardnesses. As expected, reducing T2 pressure is found to decrease the maximum contact pressure. Similarly reducing all layers hardnesses will also result in decreasing maximum contact pressure and as a consequence is expected to reduce PSM signal. The trend of the dependence on the thicknesses, however, differs between the various layers. Increasing only the softer layers thicknesses (CL and CSL) will decrease forces and thus reduce PSM. Nevertheless, for the same purpose TCL thickness should decrease. Since the TCL is the toughest layer its effect on the contact pressure is opposite. The order of importance of various layers thickness change is: CL> CSL>TCL.

The dependence of PSM formation on CSL properties has been validated by on-line press experiments. The evlution of the PSM signal on paper was graded as a function of the amount of printing impressions. This was measured for various blanket configurations. In Figure 7a we show the maximal contact pressure upon changing the (low strain) modulus of the CSL and upon changing CSL thickness. As mentioned PSM signal is reduced when CSL hardness decreases and also when its thickness increases. The effect of thickness seems to reach saturation and after ~160um no further significant changes occur. In Figure 7b and 7c we show the experimental results. In Figure 7b there are three blankets configurations, where the thicker CSL blanket shows a smaller PSM signal formation. In Figure 7c we show the effect of changing CSL hardness thus causing a further decrease in the signal. In addition, both the simulation predictions and the experimental results agree that the effect of hardness is more prominent in creating the PSM signal. Thus, changing hardness by a factor of 1.5 is much more significant to the extent of the PSM signal than changing thickness by the same factor.

(a)

(b)

(c)

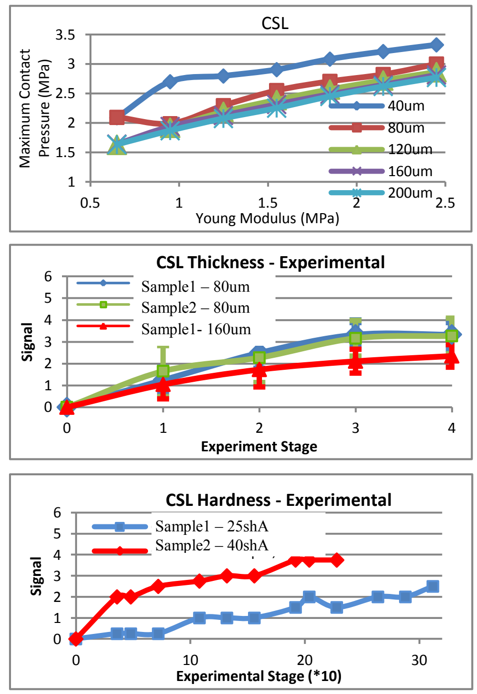

***Figure 7**. (a) Maximum contact pressure on CSL layer upon changing its thickness and hardness (b) Experimental evidence that increasing CSL thickness decreases PSM signal. (c) Experimental evidence that decreasing CSL hardness decreases PSM signal. Effect of hardness is more significant on PSM formation.*

Steady-State Rolling Model - OPC Cracks

Another failure studied is the formation of OPC cracks at T1 (see Figure 8a). Experimental evidence shows that web blankets cause much more cracks than sheet blankets. We want to understand this effect and other parameters influencing shear forces on the OPC. For this purpose further experimental analysis was done to characterize the blankets shear properties. Both sheet-fed and web blankets shear stress-strain relationships were measured and this was added to the material models of each.

In order to simulate rolling we employ steady-state transport feature of Abaqus. In this algorithm the motion is uniform under constant forces and therefore the strain field does not change in time. The algorithm uses an Eulerian - Lagrangian framework. Rigid body rotation is described in a spatial manner while mesh follows blanket deformation with rolling. Constant average velocities are imposed and a model for friction was inserted. We study parameters influencing the shear forces exerted on the OPC, where we are mainly interested in the effect of blanket shear properties. One of the simulation advantages is that it allows for studying the effect of a specific parameter, e.g. we can create a virtual blanket with only shear properties changed. Thus we can study the effect of this property on the system's behavior.

The steady-state rolling procedure gives us a snapshot of rolling behavior. Results give both local normal compressive $p(x)$ and local shear $q(x)$ tractions along the contact line sustained by friction. From the relationship between these quantities we can find the stick and slip regions in our system.

$$s(x) = 0 \qquad |q(x)|/\mu \le p(x) \tag{8}$$

$$sign[s(x) \neq 0] = -sign[q(x)] \qquad |q(x)|/\mu = p(x) \tag{9}$$

where μ is the coefficient of friction and
$s(x)$ is the local slippage.

Here we find that in most of the contact region starting from the trailing edge there is sticking where only at the leading edge there is transition to slippage. This is depicted in Figure8c where we plot $p(x)$ and $-\mu q(x)$. The local relative velocities values $s(x)$ (shown in the secondary axis) are much larger (in their absolute values) than 0 in this region and the blanket lags after the OPC.

(a) 

(b) 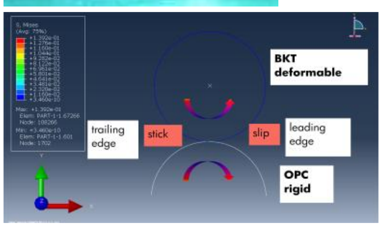

(c) 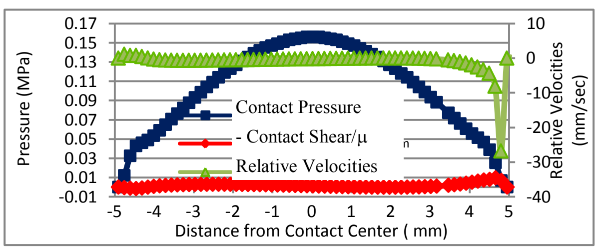

(d) 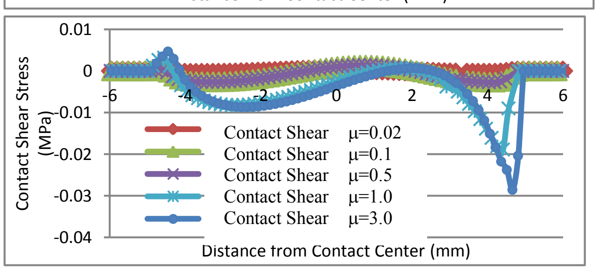

***Figure 8**. (a) A picture of OPC with cracks (b) Schematic view of the steady state rolling model with stick and slip regions (c) Contact pressure, minus contact shear stress times the coefficient of friction showing the stick to slip transition which fits the relative velocities behavior shown in the secondary axis (d) Contact shear forces upon changing the coefficient of friction showing a very sharp reduction in shear when μ becomes 0.5 and smaller.*

The transition between stick and slip is characterized by a peak in the shear force. A maximal shear force is found to be ~2 times larger for blankets with web blankets shear properties than for those having sheet shear behavior. This implies that web blankets may create more cracks than sheet blankets.

We can reduce shear forces exerted on the OPC by increasing CL layer thickness or by reducing friction between OPC and blanket. Increasing the CL layer thickness gradually decreases the peak shear stress. A different behavior is observed upon decreasing the coefficient of friction. When μ decreases to a threshold value which is 0.5 and lower, total slippage occurs and no stick region will be observed.

Several experimental features of OPC crack formation fit the simulation: they start at the leading and propagate to the trailing edge in agreement with the calculated maximal shear stress position. A thinner compressible layer was shown to induce more cracks also in correspondence with the simulation findings. Printing on an image was shown to cause less cracks than printing on background due to lower friction in the image region. This also fits the simulation results discussed before. A current solution for OPC cracks is implemented in the machines by wetting the system and thus reducing frictional effects as predicted by simulation.

Ink Dispersion Unit (IDU) Seal

Another model consists of optimization of a rubber seal used for the ink dispersion unit (IDU) designed for new machines. The initial seal configuration shown in Figure 9a did not close well and was torn. A new configuration was sought for and there was no direction known. Experimentally one would build many configurations and test their behavior in order to find the best one. However, employing the simulation we found a much more simpler, cheaper and quicker solution to this problem.

(a) 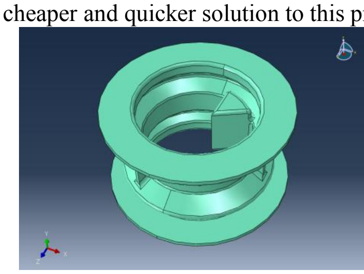

(b) 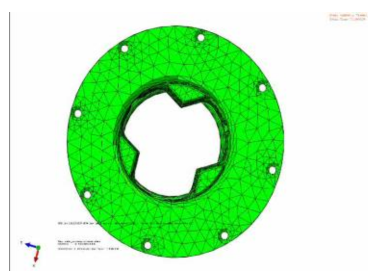

(c) 

***Figure 9**. (a) First IDU cap design sketch (b) Final design sketch (c) Real unit used in the machine. Applying pressure on the unit shows same behavior as doing the same in the model (b).*

©2014 Society for Imaging Science and Technology

In order to model correctly the material behavior of the rubber comprising the seal it was measured by Instron. In contrast to previous measurements the rubber was measured for its tension properties as for this process this is the main deformation occuring. Similar to other rubbery layers MR model was fitted. The system's top and bottom surfaces were fixed and pressure was applied to the outer surface of the seal. Over 30 configurations were simulated in attempt to find the best closing. When the Von-Mises stress exceeded a certain threshold value this indicated tear whose positions fitted the experimental findings. From the given configurations the optimal design was chosen (Figure 4b and 4c) whose behavior with time is found to be in good agreement with experiments. Only two final prototype configurations were constructed and tested. The seal which was found to be the optimal one both by simulation and by experiment is already used in the new machines.

Substrate Coating Unit Model

Substrate coating unit is required in order to improve ink transfer and to enable a wider variaty of media gamut. One important aspect of its architecture is the mechanical behavior. The system consists of two cylindrical shells composed of rubber (with seam) (Figure 10) in contact and rotating while paper is moving inside. Rubber properties are measured and it is ascribed a MR model. Simulation steps consisted of pressing, rolling and paper insertion. Due to the seam region, rolling procedure was by Abaqus Explicit simulation and not by the steady-state procedure

(a)

(b)

(c)

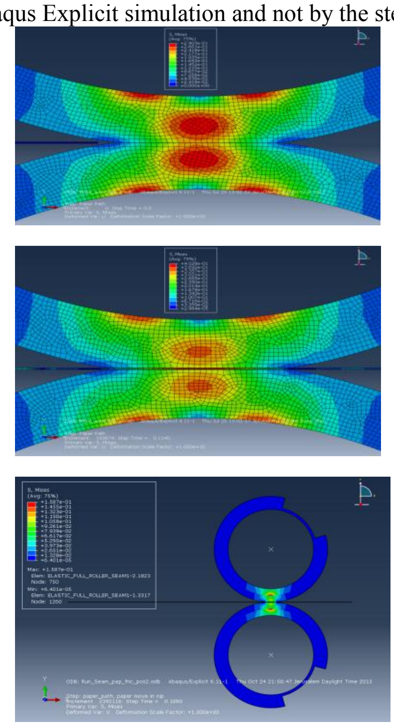

Figure 10 *Von-Mises stresses of 2 rolling cylinders: (a) alone, (b) with paper inside (c) seam and paper*

Contact pressure profiles obtained from the simulation agree with those measured by an i-scan detector and show that at low values of deflection (at the required nip length) the behavior is as predicted by Hertz model. Rolling shows a complex velocity profile in the nip area of accelarating and decelerating regions in differnet nip positions. Paper movement by drag friction allows a deeper insight at the process. This allows for optimizing the of paper transfer by understanding forces exerted on it by the rollers.

Summary and Conclusions

In this paper we have shown how the use of FEA simulations helps in optimizing mechanical systems. The models thus built give us insights and understandings of the behavior of these systems and the effect of various parameters on observed performance. Several blanket failures have been studied and their dependence on the mechanical properties was found. The modeling results have been addressed for future blanket configurations for optimization. The IDU seal model demonstrates how such an optimization can save in production and costs and predict the correct configuration before constructing the samples.

We plan to improve several features in modeling and materials properties inputs, such as time dependence and hysteresis. Further calculations consist of studying changes in the process parameters (drum sizes, velocities etc.) and finding optimal work space for the described and other machine parts development.

Acknowledgements

We thank Yossi Shachak for his help in the IDU seal configurations and Mordechai Arenson and Alex Feygelman, for their contribution to the ILP project.

References

[1] Abaqus Analysis User's manual
[2] Tyre/road friction modeling Literature survey, R. van der Steen DCT 2007.072 Eindhoven University May, 2007 and ref.
[3] E.g. J. Wu, M Nakazawa, T. Kawamura, H. Baba, H. Kamimura, N. Tanaka and K. Miyahara, JSME Int. J.42,3,(388),1999
[4] M. Safadi, W. Salalha, N. Schupper and M.B. Rubin, in preparation.
[5] K. L. Johnson, Contact mechanics, Cambridge, 2003
[6] F. Archard, Proc. Roy. Soc. of Lond, A, 243(1233):190 1957, Fund. of Tribology, R Gohar, H Rahnejat World sci 2008.

Author Biography

Nurith Schupper received her B.Sc. in chemistry and physics (1996) from the Hebrew University. She finished her M.Sc. (1999) and PhD (2005) at Bar-Ilan University in pulse propagation, light scattering from amorphous materials and in statistical and polymer physics. After this she postdoctoral studies (2006-2008) at Weizmann institute on glass transition. She is currently a physicist in materials department at the R&D Division of HP-Indigo.

Peter Forgacs has earned his PhD degree in physics from the Eotvos Science University, Budapest, Hungary in 1978 and undertook a post-doctoral training in the Polymer Research Institute at the University of Massachusetts in1982-1984. In 1989 he joined Hewlett-Packard Indigo Division, Israel, at that time Indigo Co., for managing the Laboratory of Physical Properties in the R&D Materials Science Section. His main topics of interest are rheology, adhesion, tribology, measuring techniques and surface characterization of solids.

Wael Salalha finished his PhD degree and postdoctorate in mechanical engineering at the Technion, Israel Institute of Technology in (2005) and (2007), respectively. His research fields were on Nano/Micro-Fluidics, Nanotechnology and Electrospinning of functionalized polymeric nanofibers. He worked as physicist at HP, Indigo division between 2007-2014. He currently is a physicist at Xjetsolar company.